Shell model description of the low-lying states of the neutron deficient Cd isotopes

N. Boelaert,* N. Smirnova, and K. Heyde
Department of Subatomic and Radiation Physics, Ghent University, Proeftuinstraat 86, B-9000 Ghent, Belgium

J. Jolie
Institut für Kernphysik, Universtät zu Köln, Zülpicher Straße 77, D-50937 Köln, Germany
(Received 11 August 2006; revised manuscript received 25 October 2006; published 24 January 2007)

Shell model calculations have been performed for the neutron deficient Cd nuclei from $N = 50$ through $N = 58$. The nucleus ^{88}Sr is taken to be an inert core with valence protons filling the $\{2p_{1/2}, 1g_{9/2}\}$ orbitals and neutrons the $\{2d_{5/2}, 3s_{1/2}, 2d_{3/2}, 1g_{7/2}, 1h_{11/2}\}$ orbitals. Using a realistic effective interaction, we have calculated the energy spectra and transition probabilities in ^{98,100,102,104,106}Cd. We have also made predictions about the presence of mixed-symmetry states that are in good agreement with the corresponding experimental data in ^{106}Cd.

DOI: 10.1103/PhysRevC.75.014316 PACS number(s): 21.60.Cs, 23.20.−g, 27.60.+j

The Cd isotopes are of considerable interest because they have only two protons less than the number found in the single closed shell Sn nuclei. Therefore, they form a good laboratory for the study of the transition from typical shell model properties when few valence neutrons are present to collective or even coexisting phenomena at the neutron midshell ($N = 62$).

The stable ^{110,112}Cd isotopes have been well described as collective nuclei showing multiphonon excitations of several kinds as well as collective 2p-2h excitations, leading to shape coexistence between normal and intruder states [1–3]. In particular, the description of these excitations in the framework of the interacting boson model (IBM) [4] was very successful, yielding a consistent description of nearly all observed low-lying excitations. In the lighter ^{106,108}Cd isotopes, several collective excitations can be identified [5,6], but it becomes more difficult to describe them using a consistent calculation, because of increased fragmentation with noncollective states. More neutron deficient Cd isotopes only have a few valence neutrons above the $N = 50$ shell. Therefore, one expects a smooth transition of the single-particle behavior in the very light Cd nuclei toward more collective vibrational behavior as the number of neutrons increases.

Besides the successful description of the low-lying excited collective states in the Cd isotopes around mass $A = 112$ obtained using the proton-neutron interacting boson model (IBM-2) [4], this model also predicts a new class of excitation modes: the so-called mixed-symmetry (MS) excitations. Here, the valence protons and neutrons are moving out of phase, e.g., leading to a low-lying 2^+ state which decays via a strong $M1$ transition to the first excited 2^+_1 state. In the Cd region, such a state was first identified in ^{112}Cd using inelastic neutron scattering [7], and more recently states with similar decay properties were identified in ^{108}Cd [8] and ^{106}Cd [6].

It is the purpose of this report to bridge the gap between the two proton hole structures observed in ^{98}Cd [9] and the collective structures in ^{106}Cd by performing detailed shell model calculations of the properties of low-lying states for ^{98,100,102,104,106}Cd in a unified way. As exemplified for the case of mixed-symmetry states, this will allow a detailed study of the shell model foundation of collectivity.

Calculations of the ground-state potential energy surface [10] indicate that the light Cd isotopes in the vicinity of ^{100}Sn show the expected behavior of nearly spherical nuclei. The spherical shell model approach to describing nuclear dynamics has three main ingredients: the valence spaces, the effective interaction, and the computational tools that make it possible to solve the huge secular problems involved.

In our calculations, the nucleus $^{88}_{38}Sr_{50}$ is taken to be an inert core with valence protons filling the $\{2p_{1/2}, 1g_{9/2}\}$ orbitals and valence neutrons occupying the $\{2d_{5/2}, 3s_{1/2}, 2d_{3/2}, 1g_{7/2}, 1h_{11/2}\}$ orbitals. We have used the single-particle energies from [11] (see Fig. 1).

The effective interaction used in the present study has been constructed in the following way. Our starting point was the microscopic effective interaction [12] (named here v3sb) derived from a charge-symmetry breaking nucleon-nucleon potential [13]. Using this interaction and the one from Ref. [11] (named v3rd), we carried out a systematic study of nuclei situated between $^{88}_{38}Sr_{50}$ and $^{132}_{50}Sn_{82}$. We found that both interactions describe rather well the spectroscopy of nuclei with a few valence particles (or holes), but they fail to reproduce the energy spectra for nuclei farther away from the closed shells.

These problems are well known in the construction of microscopic effective interactions based on the G matrix [14]. Their origin may well be due to the absence of the three-body forces when constructing these interactions (see, e.g., Refs. [15,16] and references therein). The largest discrepancies between experimental and theoretical energy spectra happen in particular at closed-shell (closed-subshell) nuclei and adjacent to them, where the dominant correlations are caused by the monopole term. It was proposed some time ago [14] that these deficiencies in the microscopic effective interaction be cured by empirical adjustment of its monopole part. This recipe is commonly used, and it has proved to be very successful, e.g.,

*Also at the Institut für Kernphysik, Universtät zu Köln, Zülpicher Straße 77, D-50937 Köln, Germany.

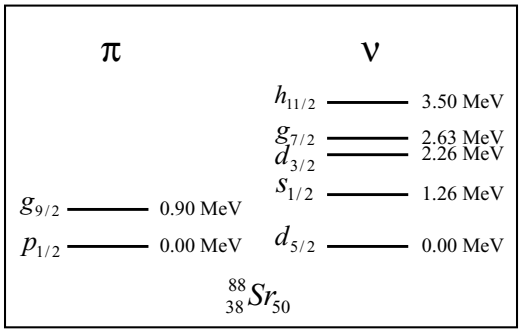

FIG. 1. Choice of the proton and neutron valence space.

for one-oscillator shell spaces beyond ^{40}Ca [14,17], ^{56}Ni, and ^{100}Sn [18], etc. These are, of course, the minimum required modifications.

There exists a different approach to deriving an effective interaction applicable in a given mass region that involves performing a least-squares fit of the two-body matrix elements to the known energy levels (e.g., Refs. [19,20]). In the present study, we followed the method outlined in Ref. [17], to which we made some modifications, mainly of the monopole part of the interaction in order to improve the overall description in the region of interest. First, the proton-proton two-body matrix elements were replaced by the empirical values from Ref. [21]. Since there are only nine matrix elements, the least-squares fit reported by Gloeckner works perfectly for $N = 50$ isotones. This is important for Cd nuclei, which contain as many as eight valence protons beyond the Sr core in the model space we are using at present. Secondly, the neutron-neutron and the proton-neutron part were slightly adjusted in order to obtain a better overall agreement with experimental data in the region. The monopole part of the interaction was modified to ensure a correct propagation of neutron single-particle energies from $N = 50$ toward $N = 82$, and we also made the pairing among the neutrons (e.g., as in Ref. [20]) slightly (0.05 MeV) more repulsive.

As a final outcome, the value of $\sigma^2 = \sum_{i=1}^{N} \frac{(E_{i,\mathrm{calc}} - E_{i,\mathrm{exp}})^2}{N}$ covering $N = 189$ data points (excitation energies) in the mass region considered has been reduced to $\sqrt{\sigma^2} = 0.354$ MeV for the interaction we use in our present study of the Cd nuclei; this value is lower than the initial value of $\sqrt{\sigma^2} = 0.437$ MeV for v3sb, our starting point, and also better than $\sqrt{\sigma^2} = 0.612$ MeV derived from the v3rd interaction from Ref. [11]. The details about the modifications and all the results will be published elsewhere [22].

The large-scale shell model calculations were carried out using the code ANTOINE [23], which is an m-scheme code based on the Lanczos algorithm through which a treatment of giant matrices becomes possible. The algorithm allows for a fast convergence when studying the lowest eigenstates for each spin, parity J^π combination.

We calculated for ^{98,100,102,104,106}Cd the lowest energy levels with spin from $J = 0$ until $J = 10$. In addition, the $B(E2)$ values between different states were calculated. We used these values to place the energy levels in bands: states with large $B(E2)$ values between them belong to the same band. By doing it this way, a comparison with the experimental level scheme becomes possible.

In progressing from ^{100}Cd toward ^{106}Cd, the occupation of the $1h_{11/2}$ orbital was rather low; so in the calculation of ^{106}Cd, we were able to impose the restriction of a maximum of two valence neutrons occupying the $1h_{11/2}$ orbital without losing precision, while achieving a large gain in computer time.

In Fig. 2, we summarize our calculations: all fitted experimental levels with known spin and parity that were used in the fitting procedure to fix the effective interaction are plotted, together with the theoretical levels. The experimental level schemes are taken from Refs. [24–27]. The effective interaction as constructed for the study of the Cd region provides very good agreement with the experimental data. Moreover, the present shell model calculations are able to describe the onset of collectivity as reflected by the $4_1^+/2_1^+$ energy ratio as given in Fig. 3. This figure clearly shows the transition from a typical shell model seniority spectrum involving the ratio 1.5 toward more collective vibrational structures.

For the calculation of the $B(E2)$ values, we used the proton and neutron effective charges which are, respectively, $1.7e$

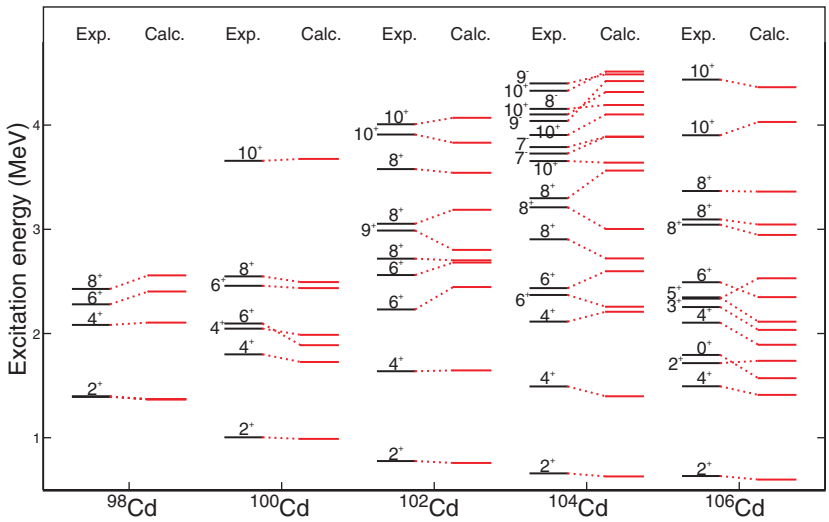

FIG. 2. (Color online) Experimental and theoretical energy spectra of ^{98,100,102,104,106}Cd used in the fit.

TABLE I. Table with experimental and theoretical $BE(2)$ values with $\{\tilde{e}_\nu, \tilde{e}_\pi\} = \{1.1, 1.7\}e$.

	E_{level} (keV)	J_i^π	E_γ (keV)	J_f^π	$B(E2)_{\text{exp}}$ (e^2 fm^4)	$B(E2)_{\text{calc}}$ (e^2 fm^4)
^{98}Cd	2428	8^+	147	6^+	49(25)[a]	49
^{100}Cd	2549	8^+	90	6^+	41(9)[b]	79
			453	6^+	0.481(32)[b]	1.6–7
^{102}Cd	777	2^+	777	0^+	562(90)[c]	540
	1638	4^+	861	2^+	>225[d]	771
	2231	6^+	593	4^+	406(27)[d]	531
	2718	8^+	487	6^+	0.17(2)[d]	51
	3053	8^+	822	6^+	485(116)[d]	471
^{104}Cd	658	2^+	658	0^+	779(27)[c]	749
	1492	4^+	834	2^+	1352(488)[c]	1073
	2370	6^+	878	4^+	>246[e]	966
	2436	6^+	322	4^+	595($^{60}_{50}$)[e]	325
			944	4^+	10.3(8)[e]	17
	2904	8^+	468	6^+	1.4(2)[e]	2.63
			533	6^+	14.7(8)[e]	1.57
^{106}Cd	633	2^+	633	0^+	749(44)[f]	883
	1494	4^+	861	2^+	1336(93)[f]	1252

[a]From Ref. [26].
[b]From Ref. [27].
[c]From Ref. [29].
[d]From Ref. [25].
[e]From Ref. [30].
[f]From Ref. [31].

and 1.1e. The effective proton charge was determined by comparing the experimentally known [26] and the calculated $B(E2)$ values of the $8_1^+ \rightarrow 6_1^+$ transition in ^{98}Cd. Because in our model space there are no valence neutrons in ^{98}Cd, the calculated $B(E2)$ values are only influenced by the effective proton charge. Once the proton charge was set, we determined the neutron charge by comparing the experimentally known and theoretically calculated $B(E2)$ values in ^{102,104}Cd. Note that the resulting effective charges are smaller than the values 1.8e and 1.5e that were used by Holt *et al.* [11]. In Table I we present a survey of the $B(E2)$ values.

In Fig. 4 we present the variation of the $B(E2; 2_1^+ \rightarrow 0_1^+)$ values, together with the separate proton and neutron contributions, with increasing neutron number. The overall trend is in line with the experimental numbers; we clearly see an increase of the $B(E2)$ values with increasing neutron number.

However, if we calculate the ratio $B(E2; 4_1^+ \rightarrow 2_1^+)/B(E2; 2_1^+ \rightarrow 0_1^+)$ in ^{102,104,106}Cd, we obtain an almost constant behavior: 1.43, 1.43, and 1.42. These values approach the vibrational U(5) ratios [28]: 1.33, 1.5, and 1.6. The corresponding O(6) values of 1.09, 1.21, and 1.27, respectively, are clearly smaller than the corresponding shell model values. It is interesting to compare them with the experimentally known ratios for ^{102,104,106}Cd, i.e., >0.4, 1.74(67), and 1.78(16), respectively.

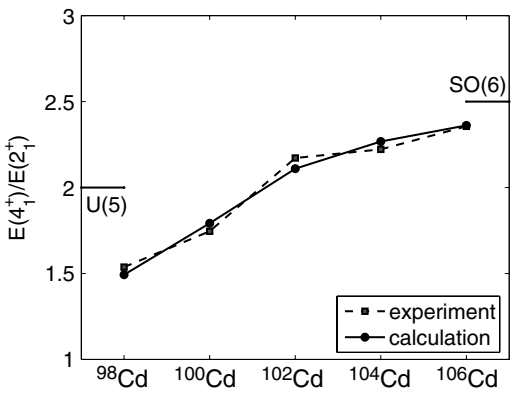

FIG. 3. Experimental and theoretical excitation energy ratios of 4_1^+ and 2_1^+ states in Cd isotopes.

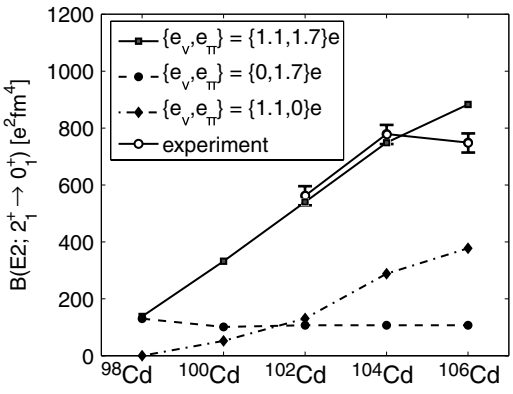

FIG. 4. Experimental and theoretical $B(E2; 2^+ \rightarrow 0^+)$ values for different Cd isotopes. Calculations were carried out with three combinations of effective charges as shown in legend.

Mixed-symmetry (MS) states have been of interest, both theoretically and experimentally [32,33], and have been described successfully within the framework of the IBM-2 [34], which predicts the lowest-lying collective states to be dominantly isoscalar excitations in the proton and neutron contributions. The IBM-2, however, also predicts a class of excitations that are nonsymmetric in the proton and neutron contributions and are called excitations with a MS character. Such states can, however, also be well understood within a shell model approach [35,36] and are likewise characterized by a mixed charge permutation symmetry of the corresponding shell model wave functions. A key signature, required to assign a state a MS character, derives from the rather specific $E2$ and $M1$ decay properties:

(i) Strong $M1$ transitions (of the order of 1 μ_N^2) to low-lying symmetric states.
(ii) Weak collective $E2$ transitions (with transition probabilities about 10% of the strong $E2$ transitions such as $2_1^+ \rightarrow 0_1^+$) to low-lying symmetric states.
(iii) Strong collective $E2$ transitions among the MS states themselves.

To locate states with a particular MS character, we first have to discuss the $E2$ and $M1$ transition operators in some detail. One can split the the $E2$ and $M1$ operator in a neutron and a proton part [37], that is,

$$O(E2) = \tilde{e}_p O(E2, p) + \tilde{e}_n O(E2, n), \tag{1}$$

$$O(M1) = \sqrt{\frac{3}{4\pi}} \sum_{i=p,n} [\tilde{g}_l(i)\mathbf{l}_i + \tilde{g}_s(i)\mathbf{s}_i]\mu_N, \tag{2}$$

with

$$O(E2, \rho) = r_\rho^2 Y_2^M(r_\rho). \tag{3}$$

By replacing $\tilde{e}_p$ and $\tilde{e}_n$ with, respectively, $(\frac{\tilde{e}_p+\tilde{e}_n}{2} + \frac{\tilde{e}_p-\tilde{e}_n}{2})$ and $(\frac{\tilde{e}_p+\tilde{e}_n}{2} - \frac{\tilde{e}_p-\tilde{e}_n}{2})$, we obtain

$$O(E2) = \frac{\tilde{e}_p + \tilde{e}_n}{2} \underbrace{(O(E2, p) + O(E2, n))}_{O(E2,s)} + \frac{\tilde{e}_p - \tilde{e}_n}{2} \underbrace{(O(E2, p) - O(E2, n))}_{O(E2,as)}. \tag{4}$$

The same procedure can now be applied for the $M1$ operator:

$$O(M1) = \sqrt{\frac{3}{4\pi}} \left\{ \underbrace{\frac{\tilde{g}_{l,p} + \tilde{g}_{l,n}}{2}(\mathbf{L}_p + \mathbf{L}_n) + \frac{\tilde{g}_{s,p} + \tilde{g}_{s,n}}{2}(\mathbf{S}_p + \mathbf{S}_n)}_{O(M1,s)} + \underbrace{\frac{\tilde{g}_{l,p} - \tilde{g}_{l,n}}{2}(\mathbf{L}_p - \mathbf{L}_n) + \frac{\tilde{g}_{s,p} - \tilde{g}_{s,n}}{2}(\mathbf{S}_p - \mathbf{S}_n)}_{O(M1,as)} \right\}, \tag{5}$$

with $\mathbf{L}_p$ ($\mathbf{S}_p$) the total proton orbital (spin) angular momentum operator and likewise for the neutron part $\mathbf{L}_n$ ($\mathbf{S}_n$). Thus, we have rewritten the operators as a sum of a symmetric (index s) and an antisymmetric (index as) part with respect to the proton and neutron interchange. Because of symmetry considerations, the contribution vanishes of the antisymmetric part of the operator to the transition probability between two states with wave functions that are either symmetric or antisymmetric in the interchange of the proton and neutron coordinates. This is also true for the contribution of the symmetric part of the operator to the transition probability between a state that is symmetric and a state that is antisymmetric in the interchange of the proton and neutron coordinates. We obtain the same behavior using states with a mixed-symmetry character.

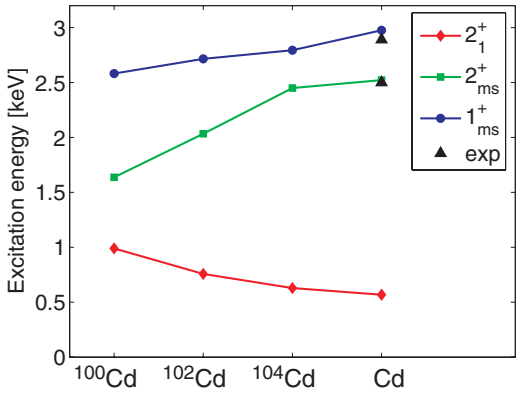

FIG. 5. (Color online) Excitation energies of $1^+_{1,\mathrm{ms}}$ and $2^+_{1,\mathrm{ms}}$ MS states together with 2^+_1 state in ^{100,102,104,106}Cd.

Considering that the effective charges are positive, so that $(\tilde{e}_p + \tilde{e}_n)$ is much bigger than $|\tilde{e}_p - \tilde{e}_n|$, and that $\tilde{g}_{l,p}$ and $\tilde{g}_{s,p}$ are positive, $\tilde{g}_{s,n}$ is negative, $g_{l,n}$ approaches 0, and $\tilde{g}_{s,p}$, $|\tilde{g}_{s,n}| > \tilde{g}_{l,p}$, so that $\tilde{g}_{s,p} - \tilde{g}_{s,n}$ is the dominant factor in Eq. (5), all properties enumerated above become obvious.

States with a MS state have been observed in quite a large number of nuclei [32,33,38]. Unfortunately, the experimental information on those states in the light Cd isotopes is limited to ^{106}Cd: a 1^+ state has recently been discovered at an excitation energy of 2.89 MeV with the characteristics of a MS state and is denoted as a $1^+_{1,\mathrm{ms}}$ state, and the presence of a 2^+ state with the decay properties of a MS state (denoted here as $2^+_{1,\mathrm{ms}}$), with a centroid at 2.5 MeV, has clearly been observed [6]. Both states are fragmented.

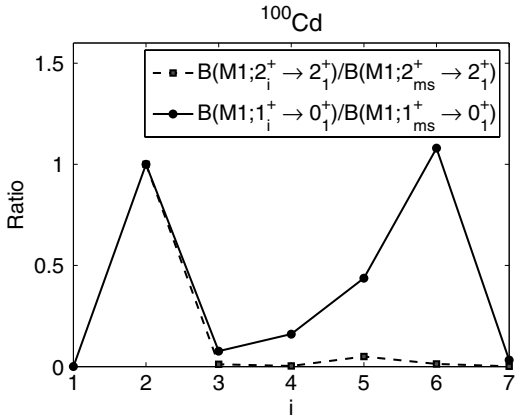

FIG. 6. $B(M1)$ ratios for the lowest 1^+_i and 2^+_i states in ^{100}Cd.

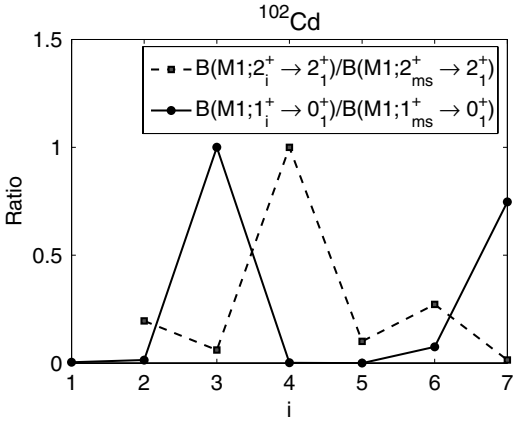

FIG. 7. Same as Fig. 6, but for ^{102}Cd.

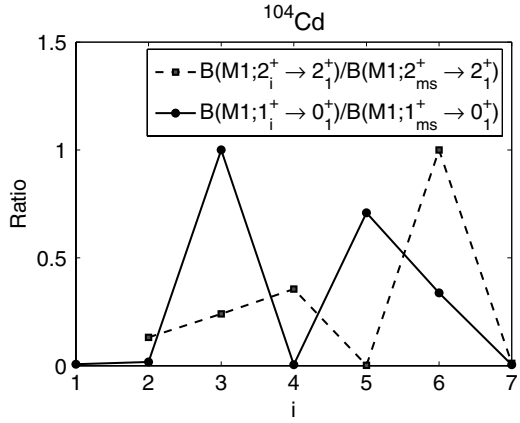

FIG. 8. Same as Fig. 6, but ^{104}Cd.

Within the shell model, it is now possible to look for states exhibiting the characteristic decay properties that characterize MS states in the light Cd isotopes, using the wave functions calculated here. We expect ^{100}Cd to be the best candidate for locating states that resemble MS states to a large extent because this nucleus is only two proton holes and two neutrons away from ^{100}Sn.

We have used the following procedure to find out if characteristics of MS states are present within the shell model: for the lowest ten 2^+ and 1^+ states, we calculated and searched for weakly collective $B(E2; 2_i^+ \to 2^+(1))$ and $B(E2; 2_i^+ \to 0^+(1))$ transitions, because transitions between mixed-symmetry 2_i^+ states and the $2^+(1)$ and $0^+(1)$ states are expected to exhibit this particular property. Then we searched for strong $B(M1; 2_i^+ \to 2^+(1))$ and $B(M1; 1_i^+ \to 0^+(1))$ jointly with a strong $B(E2)$ transition between the 2_i^+ and 1_i^+ states in order to locate candidates with a $2^+_{\rm ms}$ and $1^+_{\rm ms}$ character. For the calculation of the $B(M1)$ values, we used proton and neutron spin gyromagnetic factors that are 0.7 times the free factors. Using these conditions, we were able to map out the $M1$ and $E2$ transition probabilities and thus identify possible states that can be largely associated with MS states.

In Fig. 5 we show the results of our quest; we have plotted the excitation energies of those 1^+ and 2^+ states (which we call in the next part of the discussion the $1^+_{1,\rm ms}$ and $2^+_{1,\rm ms}$ MS states) which can be associated as well as possible with all the criteria described above that define a MS excited state, together with the energy of the 2_1^+ state in ^{100,102,104,106}Cd.

The consistency with experimental energies resulting in ^{106}Cd is striking. The typical behavior that the MS states raise in energy with increasing number of valence nucleons was observed before in the $N = 52$ nuclei [39]. The $B(E2)$ and $B(M1)$ values, extracted from all calculated values, that carry the MS character as clearly as possible, are presented in Table II. One notices, in particular, a rapid decrease of the $B(M1; 2^+_{1,\rm ms} \to 2_1^+)$ transition with increasing boson number, in contrast to the behavior for the $N = 52$ nuclei [39].

The $M1$ transitions between the MS candidates and the low-lying, mainly symmetric 0_1^+ and 2_1^+ states are not extremely strong, but the $B(M1)$ values of these transitions in comparison with those of other 1^+ and 2^+ states are notably larger. We illustrate all $B(M1)$ values for up to the seven lowest excited 2_i^+ and 1_i^+ states (with $i = 1, \ldots, 7$), expressed as ratios, for the different Cd isotopes in Figs. 6–9. In these figures, the ratios $B(M1; 2_i^+ \to 2_1^+)/B(M1; 2^+_{\rm ms} \to 2_1^+)$ and $B(M1; 1_i^+ \to 0_1^+)/B(M1; 1^+_{\rm ms} \to 0_1^+)$ are shown, giving a pictorial overview of the relative $M1$ strength distribution.

In ^{100}Cd, there appear to be two 1^+ states with a strong $M1$-transition probability to the ground state, i.e., the 1_2^+ and 1_6^+ states. Because there is no strong $E2$ transition between the 1_6^+ and the $2^+_{\rm ms}$ states, the 1_6^+ state does not contain the characteristics of a well-defined MS configuration. The same kind of arguments are used to discard the 1_7^+ and 1_5^+ states in ^{102}Cd and ^{104}Cd, respectively, as good candidates of mixed-symmetry character.

In conclusion, we have studied the transition from typical shell model toward collective properties in the light Cd nuclei using the nuclear shell model. Besides a correct reproduction of the changing energy spectra, we have noticed the onset of quadrupole collectivity as indicated by the ratio $E(4_1^+)/E(2_1^+)$

TABLE II. Theoretical $BE(2)$ values with $\{\tilde{e}_\nu, \tilde{e}_\pi\} = \{1.1, 1.7\}e$.

	^{100}Cd	^{102}Cd	^{104}Cd	^{106}Cd
$B(E2; 2^+_{1,\rm ms} \to 2_1^+)$ (e^2 fm^4)	48.0571	0.593	17.4362	25.3839
$B(E2; 2^+_{1,\rm ms} \to 0_1^+)$ (e^2 fm^4)	0.8163	0.1133	2.8811	1.9321
$B(M1; 2^+_{1,\rm ms} \to 2_1^+)$ (μ_N^2)	0.8203	0.4411	0.3227	0.0816
$B(M1; 1^+_{1,\rm ms} \to 0_1^+)$ (μ_N^2)	0.0629	0.2091	0.2211	0.1760
$B(E2; 1^+_{1,\rm ms} \to 2^+_{1,\rm ms})$ (e^2 fm^4)	562.7452	375.6672	541.6013	702.9900

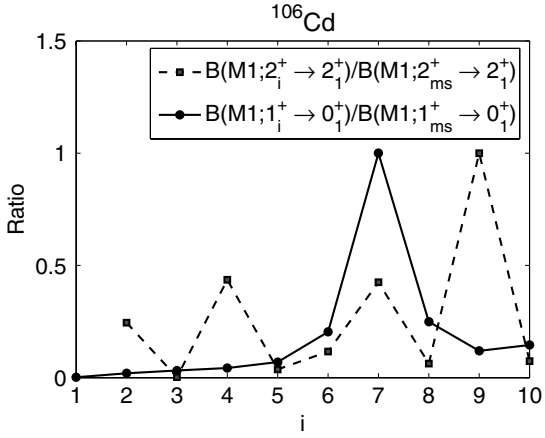

FIG. 9. Same as Fig. 6, but for ^{106}Cd.

and the $B(E2; 2_1^+ \rightarrow 0_1^+)$ value. Using the nuclear shell model, we have carried out a detailed study in order to trace excited 2^+ and 1^+ states that can be associated with a so-called mixed-symmetry character, states that are characterized by strong $M1$ transitions to the 0_1^+ and 2_1^+ states and weak $E2$ decay transition rates to these same 0_1^+ and 2_1^+ states. Thus, we have obtained a shell model underpinning of the behavior of mixed-symmetry states as appears also in a collective model approach.

N.S. thanks E. Caurier and F. Nowacki for making available their ANTOINE shell model code and for the many fruitful discussions. She also thanks M. Hjorth-Jensen for discussions about the construction of the effective interaction. This work was supported by the Inter-University Attraction Poles (IUAP) under Project P5/07 and by the Deutsche Forschungsgemeinschaft under Grant JO 391/3-2. K.H. is grateful to the FWO-Vlaanderen for financial support.

[1] J. Wood, K. Heyde, W. Nazarewicz, M. Huyse, and P. Van Duppen, Phys. Rep. **215**, 101 (1992).
[2] F. Corminboeuf, T. B. Brown, L. Genilloud, C. D. Hannant, J. Jolie, J. Kern, N. Warr, and S. W. Yates, Phys. Rev. C **63**, 014305 (2000).
[3] H. Lehmann, P. E. Garrett, J. Jolie, C. H. McGrath, M. Yeh, and S. W. Yates, Phys. Lett. **B387**, 259 (1996).
[4] F. Iachello and A. Arima, *The Interacting Boson Model* (Cambridge University Press, Cambridge, England, 1987).
[5] A. Gade, D. Belic, P. von Brentano, C. Fransen, H. von Garrel, J. Jolie, U. Kneissl, C. Kohstall, A. Linnemann, H. H. Pitz *et al.*, Phys. Rev. C **67**, 034304 (2003).
[6] A. Linnemann, Ph.D. thesis, University of Köln, 2005.
[7] P. E. Garrett, H. Lehmann, C. A. McGrath, M. Yeh, and S. W. Yates, Phys. Rev. C **54**, 2259 (1996).
[8] A. Gade, A. Fitzler, C. Fransen, J. Jolie, S. Kasemann, H. Klein, A. Linnemann, V. Werner, and P. von Brentano, Phys. Rev. C **66**, 034311 (2002).
[9] A. Blazhev, M. Gorska, H. Grawe, J. Nyberg, M. Palacz, E. Caurier, O. Dorvaux, A. Gadea, F. Nowacki *et al.*, Phys. Rev. C **69**, 064304 (2004).
[10] N. Redon, J. Meyer, M. Meyer, P. Quentin, P. Bonche, H. Flocard, and P.-H. Heenen, Phys. Rev. C **38**, 550 (1988).
[11] A. Holt, T. Engeland, M. Hjorth-Jensen, and E. Osnes, Phys. Rev. C **61**, 064318 (2000).
[12] M. Hjorth-Jensen (private communication).
[13] R. Machleidt and H. Müther, Phys. Rev. C **63**, 034005 (2001).
[14] A. Poves and A. Zuker, Phys. Rep. **70**, 235 (1981).
[15] A. P. Zuker, Phys. Rev. Lett. **90**, 042502 (2003).
[16] E. Caurier, G. Martinez-Pinedo, F. Nowacki, A. Poves, and A. P. Zuker, Rev. Mod. Phys. **77**, 427 (2005).
[17] G. Martínez-Pinedo, A. P. Zuker, A. Poves, and E. Caurier, Phys. Rev. C **55**, 187 (1997).
[18] F. Nowacki, Ph.D. thesis, IReS Strasbourg, 1996.
[19] B. A. Brown and B. H. Wildenthal, Ann. Rev. Nucl. Sci. **38**, 29 (1988).
[20] T. Otsuka, M. Honma, T. Mizusaki, N. Shimizu, and Y. Utsuno, Prog. Part. Nucl. Phys. **47**, 319 (2001).
[21] D. Gloeckner and F. Serduke, Nucl. Phys. **A220**, 477 (1973).
[22] N. Smirnova *et al.* (unpublished).
[23] E. Caurier and F. Nowacki, Acta Phys. Pol. B **30**, 705 (1999).
[24] G. de Angelis, C. Fahlander, D. Vretenar, S. Brant, A. Gadea, A. Algora, Y. Li, Q. Pan, E. Farnea, D. Bazzacco *et al.*, Phys. Rev. C **60**, 014313 (1999).
[25] K. P. Lieb, D. Kast, A. Jungclaus, I. P. Johnstone, G. de Angelis, C. Fahlander, M. de Poli, P. G. Bizzeti, A. Dewald, R. Peusquens *et al.*, Phys. Rev. C **63**, 054304 (6) (2001).
[26] M. Gorska, M. Lipoglavsek, H. Grawe, J. Nyberg, A. Atac, A. Axelsson, R. Bark, J. Blomqvist *et al.* Phys. Rev. Lett. **79**, 2415 (1997).
[27] B. Singh, Nucl. Data Sheets **81**, 1 (1997).
[28] A. Arima and F. Iachello, Ann. Phys. (NY) **99**, 253 (1976).
[29] N. Boelaert, Masters thesis, Ghent University, 2006.
[30] G. A. Müller, A. Jungclaus, O. Yordanov, E. Galindo, M. Hausmann, D. Kast, K. P. Lieb, S. Brant, V. Krstic, D. Vretenar *et al.*, Phys. Rev. C **64**, 014305 (16) (2001).
[31] M. T. Esat, D. C. Kean, R. H. Spear, and A. M. Baxter, Nucl. Phys. **A274**, 237 (1976).
[32] N. Pietralla, C. Fransen, D. Delic, P. von Brentano, C. Friesner, U. Kneissl, A. Linnemann, A. Nord, H. H. Pitz, T. Otsuka *et al.*, Phys. Rev. Lett. **83**, 1303 (4) (1999).
[33] C. Fransen, N. Pietralla, P. von Brentano, A. Dewald, J. Gableske, A. Gade, A. Lisetsky, and V. Werner, Phys. Lett. **B508**, 219 (2001).
[34] P. Van Isacker, K. Heyde, J. Jolie, and A. Sevrin, Ann. Phys. (NY) **171**, 253 (1986).
[35] K. Heyde and J. Sau, Phys. Rev. C **33**, 1050 (1986).
[36] A. Lisetsky, N. Pietralla, C. Fransen, R. Jolos, and P. von Brentano, Nucl. Phys. **A677**, 100 (2000).
[37] K. L. G. Heyde, *The Nuclear Shell Model* (Springer-Verlag, Berlin, 1994), 2nd ed.
[38] N. Pietralla, C. Fransen, P. von Brentano, A. Dewald, A. Fitzler, C. Friessner, and J. Gableske, Phys. Rev. Lett. **84**, 3775 (2000).
[39] V. Werner, D. Belic, P. von Brentano, C. Fransen, G. Gade, H. von Garrel, J. Jolie, U. Kneissl, C. Kohstall, A. Linnemann *et al.*, Phys. Lett. **B550**, 140 (2002).